International Conference on Dynamic Games, Optimal Guidance and Applications in Autonomous Systems
April 22-24, 2026, Honolulu, Hawai'i, USA

Singular Extremals of Discrete-Time Control Systems with Applications to Cellular Automata

M. Chyba*, S. Glickman#

University of Hawai'i at Mānoa
Department of Mathematics
2565 McCarthy Mall
Honolulu, HI, U.S.A.
*mchyba@math.hawaii.edu, #glickman@math.hawaii.edu

Abstract

Singular extremals play a central role in optimal control theory, as they correspond to trajectories along which first-order optimality conditions fail to determine the control uniquely and higher-order structure becomes relevant. While singular extremals have been extensively studied in continuous-time systems, comparatively little is known in the discrete-time setting. Existing results for linear, discrete systems largely date back to the early 1970s and are restricted to highly structured canonical forms, quadratic cost functionals, and specific terminal conditions. In this work, we revisit the problem of singular optimal control for linear, time-invariant, discrete systems and extend classical results beyond the canonical coordinate setting.

The present work is motivated by a broader research program on discrete-time control systems, with particular emphasis on optimal control and singular extremals. Such systems arise naturally in a variety of settings, including controlled cellular automata, as developed in earlier work [1, 2]. In this general framework, the system evolution is described by a discrete-time control system of the form $x_{k+1} = F(x_k, u_k)$, where x_k denotes the state of the system and u_k the control applied at discrete time stages. Optimal control problems are formulated by minimizing a cost functional $J(x,u) = \sum_{k=0}^{N-1} \ell_k(x_k,u_k) + \Phi(x_N)$, subject to admissibility constraints on the control sequence and terminal conditions on the state. Even for simple models, such discrete-time systems exhibit rich behavior.

As a first step toward understanding singular optimal control in this context, we focus on the linear, discrete-time case. We consider linear, time-invariant systems of the form $x_{k+1} = Ax_k + bu_k$, where $A \in \mathbb{R}^{n\times n}$, $b \in \mathbb{R}^n$, and the pair (A,b) is controllable. The cost functional is taken to be quadratic in the state, $J(x) = \sum_{k=0}^{N-1} x_k^\top Q x_k$, where $Q = (q_{ij})$ is a constant, $n \times n$, symmetric, positive-definite matrix. The system is subject to the boundary conditions $x_0 = x(0)$ and $x_N = 0$, along with the control constraints $|u_k| \leq 1$ for $0 \leq k \leq N-1$. The problem is to choose a sequence of controls $u_0, \ldots, u_{N-1}$ which minimizes the cost functional.

After a linear change of coordinates, the system can be written in a canonical form more amenable to analysis using both the discrete-time maximum principle, a well-known tool in optimal control theory, and existing results about singular extremals. Following [3], we define the Hamiltonian associated with the system dynamics and cost functional by $H(x_k, p_{k+1}, u_k) = p_{k+1}^\top (Ax_k + bu_k) - x_k^\top Q x_k$, where $p_{k+1} \in \mathbb{R}^n$ denotes the costate vector. According to the discrete maximum principle, if an optimal sequence of controls $u_0^*, \ldots, u_{N-1}^*$ exists, then the optimal control u_k^* satisfies either $u_k^* = \operatorname{sign}(b^\top p_{k+1})$, if $b^\top p_{k+1} \neq 0$ or $u_k^* \in [-1,1]$, if $b^\top p_{k+1} = 0$.

The second case corresponds to singular controls, and the corresponding state trajectories are referred to as singular arcs. The time indices k for which $b^\top p_{k+1} = 0$ are called singular stages.

We restrict to the case in which all N stages are singular, leading to totally singular extremals. In addition, and independent of whether the control is singular or nonsingular, the state and costate sequences (x_k, p_k) satisfy the Hamiltonian difference equations associated with the discrete maximum principle.

Building on the results of [3, 4], we compute the structure of totally singular arcs for linear, time-invariant, discrete systems expressed in general coordinates, without assuming that the system is initially given in canonical form. By explicitly relating a general controllable system to its canonical representation through a linear change of variables, we characterize how the structure of singular extremals transforms back to the original coordinates. Numerical simulations are used to illustrate this correspondence and to visualize the effect of the canonical transformation on the state and costate trajectories. The resulting framework is then applied to discrete control systems arising from controlled cellular automata, providing a proof of concept for the analysis of singular extremals in this broader class of discrete models.

We illustrate the proposed approach with a simplified model of wildfire propagation formulated as a controlled cellular automaton [2]. The purpose of this model is not to provide a realistic description of wildfire dynamics, but rather to demonstrate how tools from discrete-time control theory can be applied to cellular automata. More realistic wildfire models will be considered in forthcoming work. The landscape of interest is modeled as a finite, square domain partitioned into an $l \times l$ grid G. At each discrete time step k, a temperature field, defined by a map $T_k : G \to \mathbb{R}$, assigns to each cell $c_{ij} \in G$ a temperature $T_k^{ij} = T_k(c_{ij})$. The temperature evolution is modeled using a discrete, diffusion-type update inspired by a finite-difference discretization of the Laplace operator, $T_{k+1}^{ij} - T_k^{ij} = \alpha_{ij}\,\kappa\left(T_k^{i-1,j} + T_k^{i+1,j} + T_k^{i,j-1} + T_k^{i,j+1} - 4T_k^{ij}\right)$, where $\kappa > 0$ represents an overall thermal diffusivity and the coefficients $\alpha_{ij} > 0$ encode the local propensity of each cell to exchange heat with its neighbors.

Control is introduced by allowing an external intervention to modify the coefficients α_{ij} at each time step. Specifically, we set $\alpha_{ij} \mapsto \alpha_{ij} - u_k\tilde{\alpha}_{ij}$ with $u_k \in [0,1]$, where the weights $\tilde{\alpha}_{ij}$ determine the cells in which the control acts and the control's relative effectiveness. We conclude by presenting numerical simulations illustrating singular arcs in this setting.

References

[1] Beros, A., Chyba, M., Markovichenko, O. (2019). Controlled Cellular Automata. *Networks and Heterogeneous Media, 14*(1), 1-22. https://doi.org/10.3934/nhm.2019001

[2] Chyba, M., Glickman, S., Tong A. (2025). Optimal Control for Affine Discrete Systems with Applications to Epidemiological Models and Cellular Automata for Wildfire Propagation Modeling. In: Tlelo-Cuautle, E., Campos-Canton, E., Gilardi-Velazquez, H.E., Huerta-Cuellar, G. (Eds.) *Complex Systems and Their Applications, Fifth International Conference (EDIESCA 2024)* (pp. 89 - 112). Springer. https://doi.org/10.1007/978-3-031-92314-2_5

[3] Tarn, T.-J., Rao, S.K., Zaborszky, J. (1971). Singular Control of Linear-Discrete Systems. *IEEE Transactions on Automatic Control, 16*(5), 401-410. https://doi.org/10.1109/TAC.1971.1099771

[4] Zaborszky, J., Tarn, T.-J. (1972). Further Results on the Singular Control for Linear Discrete Systems. *IEEE Transactions on Automatic Control, 17*(2), 261-264. https://doi.org/10.1109/TAC.1972.1099949

Instructions for Preparing an Abstract for International Conference on Dynamic Games, Optimal Guidance and Applications in Autonomous Systems

Price Formation in Mean Field Games of Controls: Structural Comparison

T, Kosugi[*]

[*] Fukuoka Institute of Technology
Fukuoka, 811-0295, Japan
kosugi@fit.ac.jp

Abstract

Price formation models in mean field games describe situations in which a large population of agents optimizes individual costs while interacting through a market mechanism that determines the price. In such models, the equilibrium is typically characterized by a coupled system consisting of a Hamilton–Jacobi equation for the value function of the agents and a Fokker–Planck equation describing the evolution of their distribution.

This talk focuses on a price formation model introduced by Gomes–Saúde (2021) in the context of mean field games. Let $d \in \mathbb{N}$ and $T > 0$ be constants.

$$\begin{cases} -\partial_t u - \Delta u + H(\cdot,\cdot,\omega + Du) &= V & \text{in } Q_T := \mathbb{T}^d \times (0,T), \\ \partial_t m - \Delta m - \operatorname{div}(m D_\xi H(\cdot,\cdot,\omega + Du)) &= 0 & \text{in } Q_T, \\ \displaystyle\int_{\mathbb{T}^d} m D_\xi H(x,\cdot,\omega + Du)\,dx &= -q(t) & \text{in } [0,T], \\ u(\cdot,T) &= \overline{u} & \text{in } \mathbb{T}^d, \\ m(\cdot,0) &= \overline{m} & \text{in } \mathbb{T}^d, \end{cases} \tag{1}$$

where where H, V are given functions, $q = q(t)$ is a given supply function, and $\overline{u}, \overline{m}$ are given terminal and initial data. Here, $\mathbb{T}^d := \mathbb{R}^d/\mathbb{Z}^d$ denotes the d-dimensional torus. Since m represents the distribution of the agents, we assume that

$$\overline{m} \geq 0 \qquad \text{and} \qquad \int_{\mathbb{T}^d} \overline{m}(x)\,dx = 1.$$

The above system arises from an optimal control problem for agents whose dynamics depend on their trading rates. The Hamilton–Jacobi equation characterizes the value function of the agents, while the Fokker–Planck equation describes the evolution of the distribution of agents under the optimal feedback control. The price variable ω is then determined by a market clearing condition requiring that the aggregate demand of the agents coincides with a prescribed supply. This mechanism leads to the global integral constraint coupling the Hamilton–Jacobi and Fokker–Planck equations.

The above system can also be formulated as a planning problem. More precisely, the system can be interpreted as the constrained minimization problem:

$$\text{Minimize} \quad \mathscr{J}(m,a) := \iint_{Q_T} (L(a) + V(x,t))\, m\,dxdt + \int_{\mathbb{T}^d} \overline{u}(x) m(x,T)\,dx$$

subject to

$$\begin{cases} \partial_t m - \Delta m + \operatorname{div}(ma) &= 0, \\ \int_{\mathbb{T}^d} ma\,dx &= q(t), \\ m(0) &= \overline{m}. \end{cases}$$

The structural features of this model are compared with several related frameworks in the literature. In particular, the relationship with mean field games of controls and with potential mean field game formulations is discussed. As an example, we compare the present model with the price formation model studied by Bonnans–Hadikhanloo–Pfeiffer [1], which can be formulated as a potential mean field game of controls. In that model, the price is determined endogenously through the aggregate demand and appears as the gradient of a potential functional. In contrast, in the present model the price is determined by a market clearing constraint with a prescribed supply and can be interpreted as a Lagrange multiplier associated with the constraint.

The comparison highlights how different price formation mechanisms lead to distinct analytical structures for the resulting systems. In particular, the potential structure in the model of Bonnans–Hadikhanloo–Pfeiffer [1] makes variational methods natural, while in the present framework the analysis is carried out by direct PDE techniques. The results presented in this talk are based on the author's recent work [3], where existence and uniqueness of classical solutions for multidimensional price formation models are established.

References

[1] J. F. Bonnans, S. Hadikhanloo & L. Pfeiffer, Schauder estimates for a class of potential mean field games of controls, Appl. Math. Optim., **83** (3) (2021) 1431–1464.

[2] D. A. Gomes & J. Saúde, A mean-field game approach to price formation, Dyn. Games Appl., **11** (1) (2021) 29–53.

[3] S. Koike & T. Kosugi, Classical solutions of a multi-dimensional price formation via mean field games, submitted.

International Conference on Dynamic Games, Optimal Guidance and Applications in Autonomous Systems
April 22-24, 2026, Honolulu, Hawai'i, USA

Round Trip Extremal Trajectory Synthesis from Low Earth Orbit to Lunar Surface

Round Trip Extremal Trajectory Synthesis from Low Earth Orbit to Lunar Surface

Hugh K. Ishikawa[#] Dilmurat M. Azimov[*],

[#] University of Hawaii at Manoa
2540 Dole Street, Room 306A.
Honolulu, HI 96822, USA.
hughi4@hawaii.edu

[*] University of Hawaii at Manoa
2540 Dole Street, Room 201A.
Honolulu, HI 96822, USA.
azimov@hawaii.edu

Abstract

The famous Apollo 11 was the first successful space mission to take humanity onto the surface of the Moon in 1969. Since then, several more missions were successfully executing with the last landing in the early 1970's. Since then, humanity has not yet stepped foot onto the Moon. However, renewed interest in the Moon by the international community and the American Artemis missions have revitalized efforts to return to the Moon once again and to stay there.

Currently, the efforts are mostly constrained to unmanned missions to previously unexplored regions of the Moon. These efforts to land on the Moon has been met with mixed success, due to the technological difficulties of doing so. Not accounting for failures where the launch vehicle failed to launch, guidance, navigation, and control (GNC) errors have accounted for 42% of all failures. While these failures are often due to the faults of state estimation (navigation) systems, it can also be stated that the numbers of the maneuvers contribute. This work seeks to reduce the number of phases involved to reduce points of failure the GNC system in the spacecraft.

The reduction of phases is possible through calculating the extremal trajectory of the spacecraft through iteration. Trajectory is determined through backward and forward integration propagated from the landing site. Algorithms for entire round trip is shown. Entire trajectory profile is shown along with mass expenditure. Barycentric motion is assumed for ballistic cislunar transfer trajectories. Continuous thrust is assumed.

For the landing maneuver, thrust direction is chosen to be opposite to velocity. This is assumed to be nearly optimal for cases regarding landing and orbital transfers using continuous thrust. This is collaborated by the sine-cosine and bilinear tangent steering laws being proven to be nearly optimal in terms of mass expenditure by T. Yang. In this case, the costate velocity is replaced by the velocity as the costate evolves similarly to the velocity from D. Azimov and R. Bishop's research on Apollo-Class targeting and guidance. Furthermore, D. Lawden's work in optimal space trajectories has shown that collinear thrust direction to velocity also are nearly optimal.

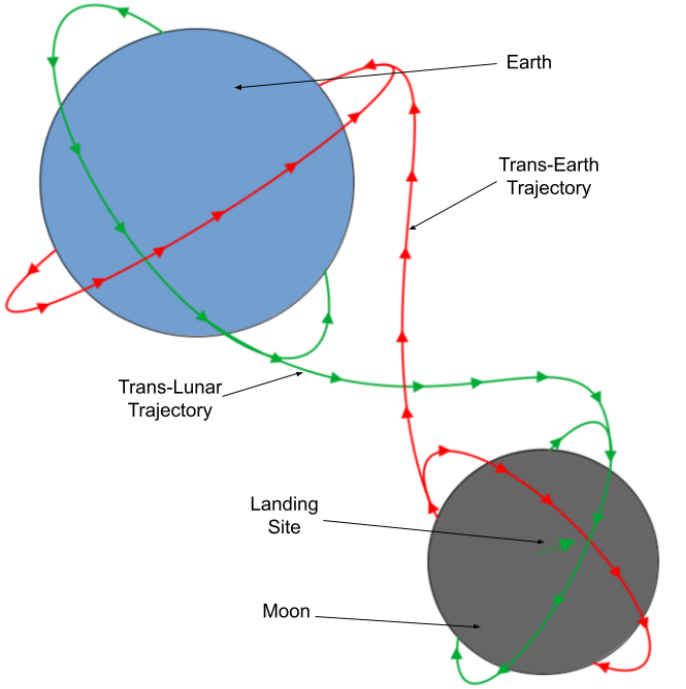

Figure 1: Full illustration of trajectory. The Trans-Earth trajectory is forward integrated and the Trans-Lunar trajectory is backward integrated to account for the movement of the Moon.

The cislunar trajectory for each landing site is entirely dependent on the orientation of lunar orbit. Lunar orbit must also be coplanar to the vector representing the landing site to achieve landing. It is entirely possible to determine a round-trip trajectory from any point on the Moon's surface utilizing algorithm.

The further simplification and generality of the Moon landing problem allows for fewer software components required in spacecraft increasing robustness. Generality of the Moon landing problem allows for future missions to explore more areas of the Moon.

Synthesis of Optimal Strategies in R. Rado's 'Lion and Man' Game

Abdulla Azamov, Nodirbek Nabiev

Institute of Mathematics,
Uzbekistan Academy of Sciences,
100174, Olmazor district, University
street, 9, Tashkent, Uzbekistan
abdulla.azamov@gmail.com

Abstract

The first substantive example of pursuit-evasion dynamic games was formulated by R. Rado in 1928. In this game, the evading point Q ("the Man") moves along the circumference of a given circle C, while the pursuing point P ("the Lion") moves without restriction over the entire circle. The points are inertia-free (the equations of motions are simple:

$$\dot{x} = u,\ \ |u| \le \rho,\ \dot{y} = v,\ \ |v| \le \sigma,\ \rho \ge \sigma.$$

By an elegant geometric construction, R. Rado showed that if the maximum speeds are equal ($\rho = \sigma$), then the pursuer can achieve equality $P = Q$. Subsequently, A.S. Besicovitch 'refuted' Rado's result by showing the evader is able to prevent the attainment of equality $P = Q$ (the beginning of the 1950's). In fact, Rado and Besicovitch considered different games: in the first case, Q moves along the boundary circle; in the second case, it moves over the entire circle. From the perspective of differential game theory, the variants of Rado and Besicovitch are completely different. In Rado's case, the phase space is three-dimensional, whereas in Besicovitch's case it is four-dimensional. After dimensionality reduction, the phase spaces are reduced to two and three dimensions, respectively.

Rado's variant was generalized to the case where the «Man's» speed exceeds that of the «Lion» by J. Flynn (1970's), and to the case of arbitrary smooth curves by A. A. Azamov and A.Sh. Kuchkarov (2009). To our knowledge, no other works address Rado's variant. Numerous works consider Besicovitch's variant; they mainly rely on a heuristic approach (i.e., without rigorous definitions or proofs). The problem of approximate solution using the method of backtracking (Paczko) has also been studied.

In the present work, a complete solution of Rado's variant (Fig. 1) is provided using the method of characteristics, based on the approach proposed by Pontryagin (1966). The phase space is the strip $0 \le r \le R$, which should be factored by the variable ϑ modulo 2π, with the base corresponding to the origin of the polar coordinates (i.e., the phase space is effectively a cone). The equations of motion in the reduced coordinates are given by

$$\frac{dr}{dt} = u_1, \qquad \frac{d\vartheta}{dt} = -\frac{u_1}{r} + \frac{v}{R}, \qquad u_1^2 + u_2^2 \le \rho^2, \qquad -\sigma \le v \le \sigma,$$

The terminal set is the point $\vartheta = 0 \bmod(2\pi),\ r = R$.

Symmetry with respect to the axis $\vartheta = 0$ allows the construction of optimal strategies to be reduced to the half $0 \le \vartheta \le \pi$. Fig. 2 shows the phase portrait of the extremal trajectories obtained by the method of characteristics, while Fig. 3 shows the portrait extended to the entire phase space, and Fig. 4 shows the extension to the whole plane (when the «Lion» can start its motion from a region outside the circle). The Bellman function is continuous and piecewise-smooth, and the extremal trajectories cover the phase space exactly once; therefore, the extremal trajectories coincide with the optimal ones.

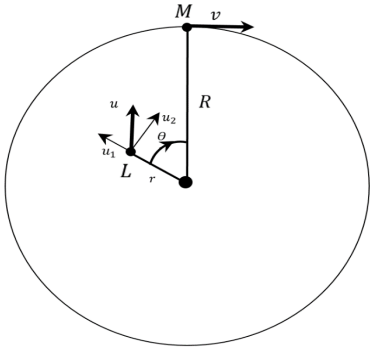

Fig.1

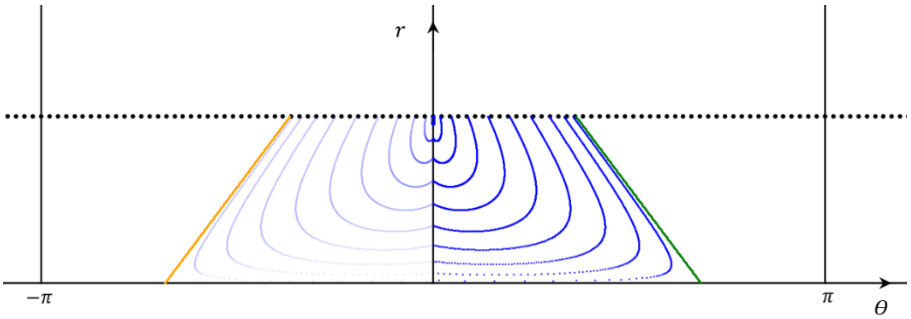

Fig.2

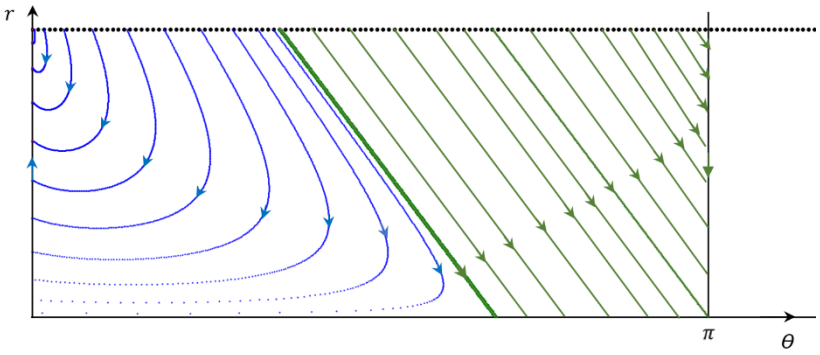

Fig.3

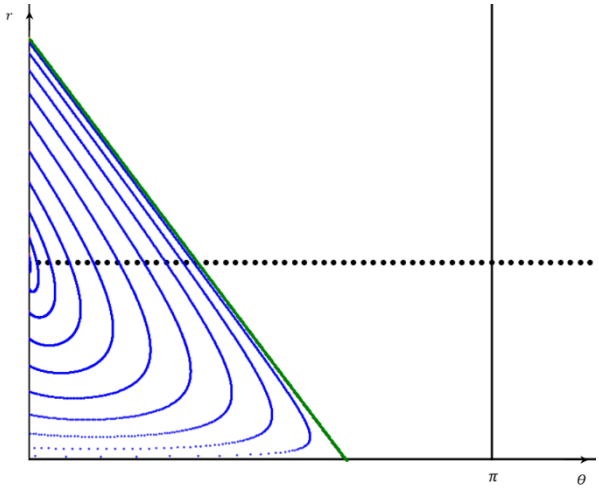

Fig.4

Real-Time Mixed-Reality-based Simulator for Autonomous Off-Road Vehicle Research

Siyuan Zhang[*1], Simran Chauhan[*2], Lorenzo Hess[*3], Nicholas Healy[*4], Sahil Gajera[*5]
Rupin R. Pradeep[#1], Alexandar Wyglinski[#2], Vladimir V. Vantsevich[*6], Lee Moradi[*7]

[*] Mechanical&Material Engineering Department
Autonomous Vehicle Mobility Institute (AVMI)
Worcester Polytechnic Institute
85 Prescott St, Worcester, USA
[*1]szhang12@wpi.edu, [*2]schauhan@wpi.edu,
[*3]lhess@wpi.edu [*4]njhealy@wpi.edu, [*5]sgajera@wpi.edu
[*6]vvantsevich@wpi.edu [*7]lmoradi@wpi.edu

[#] Electrical Engineering Department
Wireless Innovation Laboratory (WiLab)
Worcester Polytechnic Institute
100 Institute Road, Worcester, USA
rpradeep@wpi.edu
alexw@wpi.edu

Abstract

This paper presents a real-time mixed-reality-based co-simulator (Fig. 1) developed at the Autonomous Vehicle Mobility Institute, within Worcester Polytechnic Institute, to provide a next-generation modeling and simulation (M&S) solution for designing autonomous off-road vehicle systems. The simulation framework integrates physics-based virtual realities developed in Unreal Engine 5 with a ROS2-based autonomy stack, enabling real-time simulation and virtualization of vehicle dynamics, perception, planning, and control algorithms within a unified virtual environment (Fig. 1a–b).

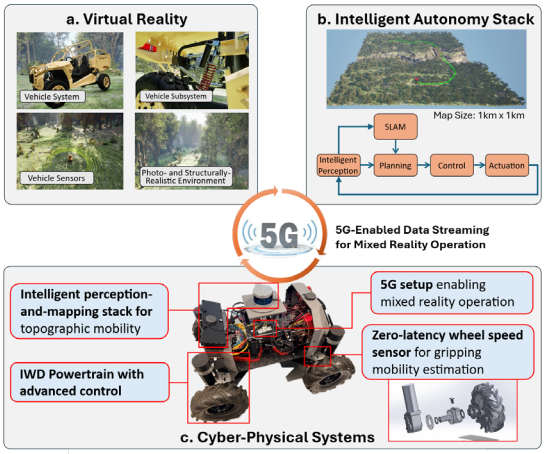

Figure 1. Overall structure of the entire system

Moreover, through a 5G-enabled communication module, the virtual realities are synchronized with a physical autonomous off-road vehicle equipped with advanced sensing and onboard control units (Fig. 1c), forming a closed-loop mixed-reality system. This architecture supports low-latency, bidirectional data exchange between simulated and physical domains, enabling real-time interaction and co-evolution of virtual and real subsystems.

This paper will present four key demonstrated capabilities of this simulator:

1. real-time co-simulation, enabling real-time execution of a complete autonomous off-road vehicle model while maintaining synchronized operation between virtual and physical platforms;
2. modular subsystem integration, enabling users to seamlessly incorporate and evaluate customized modules—such as perception, planning, or control—within a complete autonomous vehicle framework without developing the remaining subsystems;
3. generation of exteroceptive sensor data, enabling the development, training, and performance evaluation of perception systems using high-fidelity synthetic camera images and LiDAR point clouds, and
4. sensor augmentation, where synthetic perception data generated in simulation are fused with real sensor measurements to expand testing scenarios and improve robustness under diverse environmental conditions.

This co-simulation architecture establishes a mixed-reality platform that enables physics-based and data-driven modeling and simulation of autonomous vehicles in off-road conditions.

The authors acknowledge the financial support from the Massachusetts Technology Collaborative (MassTech) for supporting the development of the mixed-reality autonomous vehicle testbed at the Autonomous Vehicle Mobility Institute (AVMI), Worcester Polytechnic Institute. Their support was instrumental in enabling the integration of cyber-physical simulation capabilities presented in this work.

International Conference on Dynamic Games, Optimal Guidance and Applications in Autonomous Systems
April 22-24, 2026, Honolulu, Hawai'i, USA

Parallel Guidance Problem in Dynamic Games

Bahrom T. Samatov[*], **Dilmurat M. Azimov**[#], **Bahodirjon I. Juraev**[†]

[*] Institute of Mathematics at the Academy of Sciences of the Republic of Uzbekistan,
University str., 9, Tashkent, 100174, Uzbekistan and
Andijan State University, 129, University str., Andijan, 170100, Uzbekistan,
samatov57@gmail.com

[#] University of Hawaii at Manoa,
2540 Dole Street, Holmes 202A. Honolulu, HI, 96822, USA and
"Tashkent Institute of Irrigation and Agricultural Mechanization Engineers" National
Research University, 39 Kori Niyazov Street, Tashkent, 100000, Uzbekistan
azimov@hawaii.edu

[†] Andijan State University,
129, University str., Andijan, 170100, Uzbekistan
jbahodirjon@bk.ru

Abstract

Guidance Theory has been extensively studied in a number of studies on optimal trajectories for spacecraft, missiles and other vehicles. However, for Dynamic Systems with Conflicting Control actions (Dynamic Games Theory), this theory remains understudied. This article is devoted to the study of such problems.This paper considers two objects (e.g., aircrafts) moving under the influence of various external forces affecting their acceleration. The goal of the first object (the Pursuer) is to reach the second object (the Evader, or Target) within a given distance. Based on information about the discrete states of the Evader and the current force field of the Pursuer, a strategy is developed that allows the Pursuer to reach its goal. This problem is solved using parallel guidance by the Pursuer toward the Target (abbreviated as Π-Guidance). To solve this problem, an algorithm for stepwise parallel approach of the objects and an efficient method for calculating the completion time are proposed.

Let the inertial objects **P** (Pursuer) and **E** (Evader) be defined in space $\mathbb{R}^n$ and their motion be described by the following equations:

$$\mathbf{P}: \ \ddot{\mathbf{p}} = \mathbf{u}(t) + \mathbf{F}_P(t,\mathbf{p}), \ t \geq 0, \ \mathbf{p}(0) = \mathbf{p}_{01}, \ \dot{\mathbf{p}}(0) = \mathbf{p}_{02}, \tag{1}$$

$$\mathbf{E}: \ \ddot{\mathbf{e}} = \mathbf{v}(t) + \mathbf{F}_E(t,\mathbf{e}), \ t \geq 0, \ \mathbf{e}(0) = \mathbf{e}_{01}, \ \dot{\mathbf{e}}(0) = \mathbf{e}_{02}, \tag{2}$$

where $\mathbf{p},\mathbf{e}$ are the current states of **P** and **E** in the space $\mathbb{R}^n$; $\mathbf{p}_{01},\mathbf{e}_{01} \in \mathbb{R}^n$ and $\mathbf{p}_{02},\mathbf{e}_{02} \in \mathbb{R}^n$ are the initial states and initial velocities of the objects; $\mathbf{F}_P(t,\mathbf{p})$ is the external force acting on the acceleration of the object **P**; $\mathbf{F}_E(t,\mathbf{e})$ is the external force acting on the acceleration of the object **E**; $\mathbf{u}(t)$, $\mathbf{v}(t)$ are the control functions of objects **P** and **E**, respectively.

Let the functions $\mathbf{F}_P(t,\mathbf{p})$ and $\mathbf{F}_E(t,\mathbf{e})$ satisfy the following conditions: 1. The Caratheodory conditions: measurability in time $t \geq 0$ and continuous with respect to variables $\mathbf{p},\mathbf{e} \in \mathbf{D}$ respectively, where **D** is a given compact set from $\mathbb{R}^n$; 2. Boundedness of external force actions in domain $[0,+\infty) \times \mathbf{D}$:

$$\|\mathbf{F}_P(t,\mathbf{p})\| \leq M, \quad \|\mathbf{F}_E(t,\mathbf{e})\| \leq N, \tag{3}$$

where M, N are given non-negative numbers and $\|\cdot\|$ is the Euclidean norm in $\mathbb{R}^n$. Let the measurable functions $\mathbf{u}(t)$, $\mathbf{v}(t)$ are satisfying the conditions:

$$\|\mathbf{u}(t)\| \leq \rho, \quad \|\mathbf{v}(t)\| \leq \sigma, \text{ for almost all } t \geq 0, \tag{4}$$

where ρ, σ are non-negative parametric numbers denoting the maximum values of accelerations. A measurable function $\mathbf{u}(\cdot)$ satisfying condition (4) will be called an admissible Pursuer's control, and the set of all such controls will be denoted by $\mathbf{U}$. A measurable function $\mathbf{v}(\cdot)$ satisfying condition (4) will be called admissible Evader's control, and the set of all such controls will be denoted by $\mathbf{V}$.

Suppose that at the initial time $t = 0$ the inequality $\|\mathbf{p}_{01} - \mathbf{e}_{01}\| > l$ holds, and the pursuer's goal is to reach the evader's l-neighborhood in finite time, where l is a given positive number. The Guidance Problem is defined as finding a way to guide the Pursuer parallel to some l-neighborhood of the Evader. The Evader's goal is to prevent the Pursuer from approaching the l-neighborhood for all $t \geq 0$ or to avoid l-capture. Finding conditions under which evasion from l-capture assumed is possible is called the l-Evasion Problem.

To solve the problem, the following steps were completed:

1. For each step, the parallel guidance of the Pursuer is determined, and it is constructed solely based on the last three phase states of the Evader and the current external influences on the Pursuer;

2. Key properties of the parallel guidance strategy are investigated;

3. The distance between the pursued and evading objects is estimated;

4. The guaranteed step for completing the guidance process to the l-neighborhood of the Evader is determined.

The following main statement is proved in the paper.

Theorem. If in the Guidance Problem (1)–(4) $\rho > \gamma$, $\|\mathbf{p}_{01} - \mathbf{e}_{01}\| > l$, then the Pursuer can reach the l-neighborhood of the Evader no later than time $T(\varepsilon)$, $0 < \varepsilon < \sqrt{\frac{a-l}{2\beta}}$ for arbitrary control $\mathbf{v}(\cdot) \in \mathbf{V}$, where

$$T(\varepsilon) = \frac{1}{\alpha}\left(\frac{b}{2} + \varepsilon\beta + \sqrt{(\frac{b}{2} + \varepsilon\beta)^2 + \alpha(a - l - 2\varepsilon^2\beta)}\right),$$

$a = \|\mathbf{p}_{01} - \mathbf{e}_{01}\|$, $b = \|\mathbf{p}_{02} - \mathbf{e}_{02}\|$, $\alpha = (\rho - \gamma)/2$, $\beta = \sigma + N, \gamma = \sigma + N + M$.

Robust Control of an Inverted Pendulum Under Noisy Conditions Using LQR and Kalman Filtering

Kevin R. Anderson[*], Ryan Okerson[*]

[*] Calif. State Polytechnic University,
Mechanical Engineering
3801 West Temple Ave, Pomona, CA
USA
kranderson1@cpp.edu

Abstract

Attitude control concerns the orientation of a body in space and is a fundamental problem in aeronautical and aerospace engineering, with applications ranging from rocket stabilization and aircraft flight control to satellite orientation. Such systems rely on sensors and actuators, which directly influence system observability and controllability through their effects on the state-space representation. A classic benchmark for studying attitude control is the inverted pendulum on a cart, a nonlinear, multi-dimensional system well suited for investigating modern state-space control and estimation techniques.

This work examines the implementation of an optimal state-space controller for a one-degree-of-freedom inverted pendulum as shown in Figure 1 using a discrete-time Kalman filter and a Linear Quadratic Regulator (LQR) as showin in Figure 2. Herein, MATLAB simulations are used to model the system, incorporate process and measurement noise, and evaluate control performance. The Kalman filter serves as a predictor–corrector state estimator, mitigating the detrimental effects of noise amplification inherent in feedback control systems. Controller gains are obtained by minimizing a quadratic cost function that balances state regulation against actuator effort, with weighting matrices selected empirically to ensure stability while respecting actuator limitations.

Simulation results demonstrate that the Kalman filter provides accurate, smooth state estimates that closely track system dynamics, enabling effective feedback control even under significant noise and external disturbances. Step perturbations applied to the pendulum velocity confirm the system's ability to recover and maintain stability. Overall, the combined LQR–Kalman framework significantly improves system robustness and performance, highlighting the importance of optimal state estimation in practical attitude control applications. Typical results of the simulations are shown in Figure 3. It is important to note that the Kalman filter allows us to estimate all states of the system.

Without knowledge of all states the feedback matrix would not return favorable controls. Thus, a guess of the states must be made. Use of the Kalman filter provides the optimum estimate. As can be seen from Figure 3, the Kalman filter smoothes out measurement noise and very closely predicts the state of the system. Generally speaking, taking a measurement improves the estimate. Also, the Kalman filter estimate lags a few time steps behind actual system dynamics.

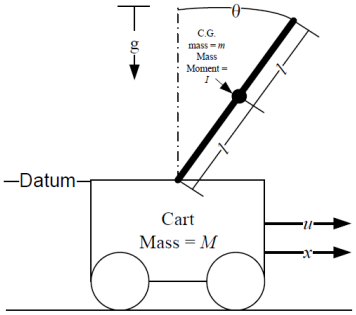

Figure 1. Inverted pendulum on a cart

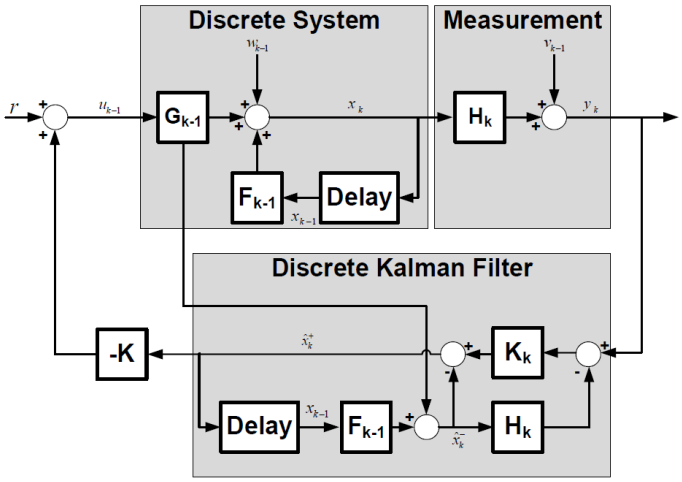

Figure 2. Kalman Filter implementation for optimal state prediction in use of a feedback system

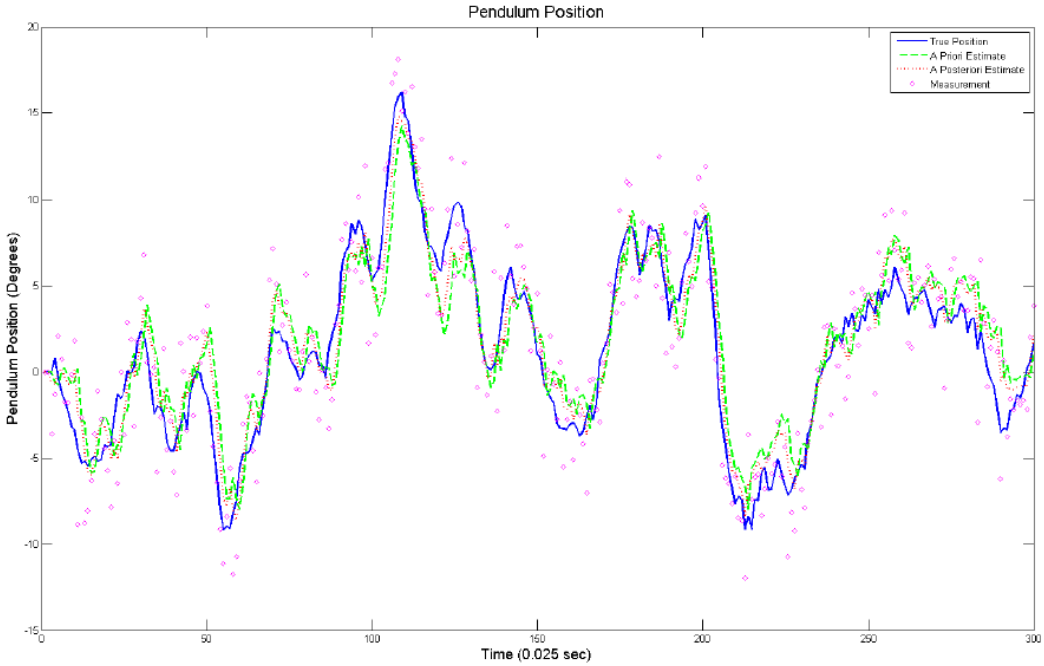

Figure 3. Simulation results showing pendulum position estimation using Kalman filter

Π-Strategy Applications in a Pursuit Game for the Pontryagin Control Example

Ulmasjon B. Soyibboev*

* Institute of Mathematics at the Academy of Sciences of the Republic of Uzbekistan,
University str., 9, Tashkent, 100174, Uzbekistan
ulmasjonsoyibboev@gmail.com

Abstract

The work is devoted to the complete study of two players pursuit differential game for Pontryagin's control example when both players possess identical motion dynamics. The pursuit problem is explored by dividing it into two separate cases, and each of them is addressed with the help of an analogue of the parallel pursuit strategy.

Let one inertial player **E** (the evader) be chased by another inertial player **P** (the pursuer) in the space $\mathbf{R}^n$. If $\mathbf{y}$ and $\mathbf{x}$ ($\mathbf{v}$ and $\mathbf{u}$) designate their position vectors (their controls), respectively, then their movements are generated by the following equations and initial conditions:

$$\mathbf{P}: \quad \ddot{\mathbf{x}} + \lambda \dot{\mathbf{x}} = \mathbf{u}, \quad \mathbf{x}(0) = \mathbf{x}_{p_0}, \quad \dot{\mathbf{x}}(0) = \mathbf{x}_{v_0}, \tag{1}$$

$$\mathbf{E}: \quad \ddot{\mathbf{y}} + \lambda \dot{\mathbf{y}} = \mathbf{v}, \quad \mathbf{y}(0) = \mathbf{y}_{p_0}, \quad \dot{\mathbf{y}}(0) = \mathbf{y}_{v_0}, \tag{2}$$

where $\mathbf{x}_{p_0}, \mathbf{y}_{p_0} \in \mathbf{R}^n$ are players' initial position vectors; $\mathbf{x}_{v_0}, \mathbf{y}_{v_0} \in \mathbf{R}^n$ are their initial velocity vectors at the time instant $t = 0$.

In Eqs.(1)–(2), the constant λ ($\lambda > 0$) is a friction coefficient of players' movements. Wherein the temporal changes of the vectors $\mathbf{u}$ and $\mathbf{v}$ are required to be measurable functions $\mathbf{u}(\cdot) : [0, \infty) \to \mathbf{R}^n$ and $\mathbf{v}(\cdot) : [0, \infty) \to \mathbf{R}^n$, they satisfy the constraints $|\mathbf{u}(t)| \leq \alpha$ and $|\mathbf{v}(t)| \leq \beta$ for almost all t, $t \geq 0$, where α and β are non-negative parametric numbers defining the maximum values of players' accelerations.

Pursuer's aim is to net the evader, i.e. to gain the relation $\mathbf{x}(T) = \mathbf{y}(T)$ in the shortest possible time $T > 0$, and evader's target is to avoid being caught, i.e. to realize the inequality $\mathbf{x}(t) \neq \mathbf{y}(t)$ at any time moment $t \geq 0$, and if this is impossible, then it tries to push back the moment of the meeting longer.

The pursuit game problem will be investigated depending on the initial data $\mathbf{z}_{p_0}$ and $\mathbf{z}_{v_0}$, where $\mathbf{z}_{p_0} = \mathbf{x}_{p_0} - \mathbf{y}_{p_0}$ and $\mathbf{z}_{v_0} = \mathbf{x}_{v_0} - \mathbf{y}_{v_0}$. Note that here only two cases are possible:

Case 1. The initial vectors $\mathbf{z}_{p_0}$ and $\mathbf{z}_{v_0}$ are collinear, i.e. there exists such a finite number μ, $\mu \in \mathbf{R}$, that the relation $\mathbf{z}_{v_0} = \mu \mathbf{z}_{p_0}$ is satisfied.

Case 2. The initial vectors $\mathbf{z}_{p_0}$ and $\mathbf{z}_{v_0}$ are non-collinear, i.e. linearly independent.

Definition 1. Set $\mathbf{z}_{v_0} = \mu \mathbf{z}_{p_0}$. Then for $\alpha \geq \beta$, the control

$$\mathbf{u}_1(\mathbf{v}, \mathbf{z}_{p_0}) = \mathbf{v} - \phi_1(\mathbf{v}, \mathbf{z}_{p_0}) \xi_{p_0} \tag{3}$$

is said to be Π–*strategy of the pursuer* in Case 1, where

$$\phi_1(\mathbf{v}, \mathbf{z}_{p_0}) = \langle \mathbf{v}, \xi_{p_0} \rangle + \sqrt{\langle \mathbf{v}, \xi_{p_0} \rangle^2 + \alpha^2 - |\mathbf{v}|^2}, \quad \xi_{p_0} = \frac{\mathbf{z}_{p_0}}{|\mathbf{z}_{p_0}|},$$

and $\langle \mathbf{v}, \xi_{p_0} \rangle$ denotes the inner product of vectors $\mathbf{v}$ and ξ_{p_0} in $\mathbf{R}^n$.

Theorem 1 (Case 1). Let: a) $\alpha = \beta,\ \mu < -\lambda$; b) $\alpha > \beta,\ \mu \in \mathbf{R}$. Then by applying Π–strategy (3), it is possible to complete the pursuit in the time interval $[0, t_1]$, where

$$t_1 = \begin{cases} \frac{1}{\lambda} \ln\big(\mu/(\lambda+\mu)\big) \quad \text{if } \ \alpha = \beta,\ \ \mu < -\lambda, \\ \\ \text{the first positive root of equation:} \\ \big(\big(\alpha - \beta + \lambda\mu|\mathbf{z}_{p_0}|\big)/\lambda^2|\mathbf{z}_{p_0}|\big)\big(1 - e^{-\lambda t}\big) - \big((\alpha-\beta)/\lambda|\mathbf{z}_{p_0}|\big)t + 1 = 0 \quad \text{if } \ \alpha > \beta,\ \ \mu \in \mathbf{R}. \end{cases}$$

Theorem 2. If $\alpha > \beta$, then in Case 1, for all $t \in [0, t_1]$ the inclusion

$$\mathbf{y}(t) \in \mathbf{M}_{p_0} + \Big(\frac{1 - e^{-\lambda t}}{\lambda}\Big)\mathbf{M}_{v_0}$$

is valid, where

$$\mathbf{M}_{p_0} = \left\{\mathbf{w} : |\mathbf{w} - \mathbf{x}_{p_0}| \geq \frac{\alpha}{\beta}|\mathbf{w} - \mathbf{y}_{p_0}|\right\}, \quad \mathbf{M}_{v_0} = \left\{\mathbf{w} : |\mathbf{w} - \mathbf{x}_{v_0}| \geq \frac{\alpha}{\beta}|\mathbf{w} - \mathbf{y}_{v_0}|\right\},$$

which are the *balls of Apollonius*.

Theorem 3 (Case 2). Let the initial vectors $\mathbf{z}_{p_0}$ and $\mathbf{z}_{v_0}$ are non-collinear. If $\alpha > \beta$, then pursuit can be terminated in differential game (1)–(2) in the time interval $[t_2, t_3]$, where

$$t_2 = \frac{1}{\lambda}\ln\left(1 + \frac{\lambda|\mathbf{z}_{v_0}|}{\alpha+\beta}\right) + \sqrt{\frac{2\mathbf{D}_1(\mathbf{z}_{p_0}, \mathbf{z}_{v_0})}{\alpha+\beta}}, \quad t_3 = \frac{1}{\lambda}\ln\left(1 + \frac{\lambda|\mathbf{z}_{v_0}|}{\alpha-\beta}\right) + \sqrt{\frac{2\mathbf{D}_2(\mathbf{z}_{p_0}, \mathbf{z}_{v_0})}{\alpha-\beta}},$$

$$\mathbf{D}_1 = \begin{cases} |\mathbf{z}_{p_0}| & \text{if } \ \langle \mathbf{z}_{p_0}, \mathbf{z}_{v_0} \rangle > 0, \\ \\ \Big|\mathbf{z}_{p_0} - \big(\langle \mathbf{z}_{p_0}, \mathbf{z}_{v_0} \rangle / |\mathbf{z}_{v_0}|^2\big)\,\mathbf{z}_{v_0}\Big| & \text{if } \ \langle \mathbf{z}_{p_0}, \mathbf{z}_{v_0} \rangle < 0, \end{cases}$$

$$\mathbf{D}_2 = \begin{cases} \big|\mathbf{z}_{p_0} + k\mathbf{z}_{v_0}\big| & \text{if } \ \langle \mathbf{z}_{p_0}, \mathbf{z}_{v_0} \rangle > 0, \\ \\ \max\big\{|\mathbf{z}_{p_0}|,\ \big|\mathbf{z}_{p_0} + k\mathbf{z}_{v_0}\big|\big\} & \text{if } \ \langle \mathbf{z}_{p_0}, \mathbf{z}_{v_0} \rangle < 0, \end{cases}$$

$$k = \frac{1}{\lambda}\Big[1 - \big((\alpha-\beta)/\lambda|\mathbf{z}_{v_0}|\big)\ln\Big(1 + \big(\lambda|\mathbf{z}_{v_0}|/(\alpha-\beta)\big)\Big)\Big].$$